

O/Rh(100) $p(2 \times 2) \rightarrow c(2 \times 2)$ order-disorder phase transition

A. Baraldi, V. R. Dhanak,* G. Comelli,† K. C. Prince, and R. Rosei†
Sincrotrone Trieste Società Consortile per Azioni, Padriciano 99, 34012 Trieste, Italy

(Received 15 May 1995)

An order-disorder transition of oxygen adsorbed on the Rh(100) surface has been studied by means of spot profile analysis low-energy electron diffraction (SPA-LEED). The $p(2 \times 2) \rightarrow c(2 \times 2)$ transition has been found to belong to the Ising universality class, with critical temperature 450 ± 5 K. Careful consideration of the profile broadening allows the determination of the type of defect implicated in the disordering process, and it is defined in terms of a surface Burgers vector. Furthermore, the thermodynamic parameters allow an energy/unit length to be associated with these defects.

I. INTRODUCTION

Oxygen on Rh(100) has been studied by several groups, and three low-energy electron-diffraction (LEED) patterns have been reported: $p(2 \times 2)$, $c(2 \times 2)$, and $p4g$.¹⁻⁸ This last structure was not observed in early work, but is known to be sensitive to the presence of impurities and surface disorder.⁹ It was originally assigned to the space group pgg by Oed *et al.*,² but the LEED pattern due to two domains of a pgg structure is indistinguishable from a single domain of $p4g$. Recent scanning tunneling microscopy (STM) work has confirmed that it is in fact $p4g$.⁸ In the present work we are concerned with a phase transition between the $p(2 \times 2)$ and $c(2 \times 2)$ structures.

The field of two-dimensional (2D) phase transitions on surfaces has been reviewed by Bauer¹⁰ and Persson,¹¹ among others. In a second-order transition, an order parameter goes continuously to zero and vanishes at some critical temperature T_c . At this temperature, the free energy for creation of a particular defect vanishes, and it is the proliferation of defects which causes the loss of order.

Although long-range order disappears, short-range order remains,¹² and is observable as residual diffraction intensity. This structural model was proposed by Schneider and Stoll,¹³ and is now generally accepted. In a recent review, Persson¹¹ illustrated a structure which consists of ordered regions of the low-temperature phase separated by well-defined boundaries or defects. The diffraction spots are of course broadened as the ordered domains are small. Only in a few cases have the types of defect been identified: they cannot be pointlike defects, as these do not destroy long-range order. Instead, they must be extended defects, which can be classified by associating a Burgers vector with them. This has been done by Prince *et al.*¹⁴ for the case of the Au(110) $(1 \times 2) \rightarrow (1 \times 1)$ (Ref. 12) and O/Rh(110) $(2 \times 2)pgm \rightarrow (1 \times 2)$ (Ref. 15) transitions.

Another approach to identifying the type of defect associated with the loss of order is to consider the possible equivalent sublattices of a system.¹¹ The transfer of an atom from one sublattice to another is regarded as a fundamental excitation of the system with which an energy is associated. We will return to this point in the analysis of the data below.

It should also be noted that the fractional-order spots may also shift from the Bragg position during disordering. This

has been described in detail by Fenter and Lu¹⁶ for a substrate of rectangular symmetry, and provides further information about the nature of the defects involved in disordering.

One of the achievements of the study of second-order transitions has been the classification of systems into universality classes, and these have been conveniently listed by Bauer.¹⁰ The first example of a surface phase transition belonging to the 2D Ising universality class was reported by Campuzano *et al.* for a clean surface,¹² and by Wang and Lu for a chemisorbed layer,¹⁷ while the first example of a three-state Potts transition was O/Ni(111).¹⁸ Within a universality class, measured quantities such as intensity and peak width vary with temperature as a power law with well-defined exponents. The point-group symmetry of the present system, O/Rh(100), is C_{4v} for the three adsorbate-induced structures which have been observed. This implies that the possible universality classes are the Heisenberg XY class with cubic anisotropy (nonuniversal exponents) or the Ising class (which is the special case of the n -state Potts model, with $n=2$). Furthermore, phase transitions between structures belonging to certain pairs of space groups cannot be second order: well-defined "selection rules" have been stated by Deonarine and Birman.¹⁹ For the present system, the high-temperature, high-symmetry phase must have a unit cell with half the area of the low-temperature phase.

II. EXPERIMENT

The experiments were carried out in a mu-metal UHV chamber pumped by a combination of turbo and ion pumps, maintaining a base pressure better than 8×10^{-11} mbar. The chamber is equipped with an Omicron spot profile analysis (SPA)-LEED, based on the design of Henzler,²⁰ which allows the measurement of LEED spot intensity profiles. The use of a channel electron multiplier, mounted behind a 100- μm aperture, in a flat screen, makes it possible to use an electron-beam current of less than 0.1 μA , minimizing damage to the adsorbate layer under investigation. An electrostatic octopole field is used to deflect the pattern into the multiplier, with a deflection range of $\pm 30^\circ$ and an angular resolution of 0.1° . The transfer width of the apparatus is better than 700 \AA at an energy of 115 eV.²¹

The sample was cleaned by cycles of Ar^+ bombardment at 3 keV and 570 K, and annealing in oxygen (10 min at

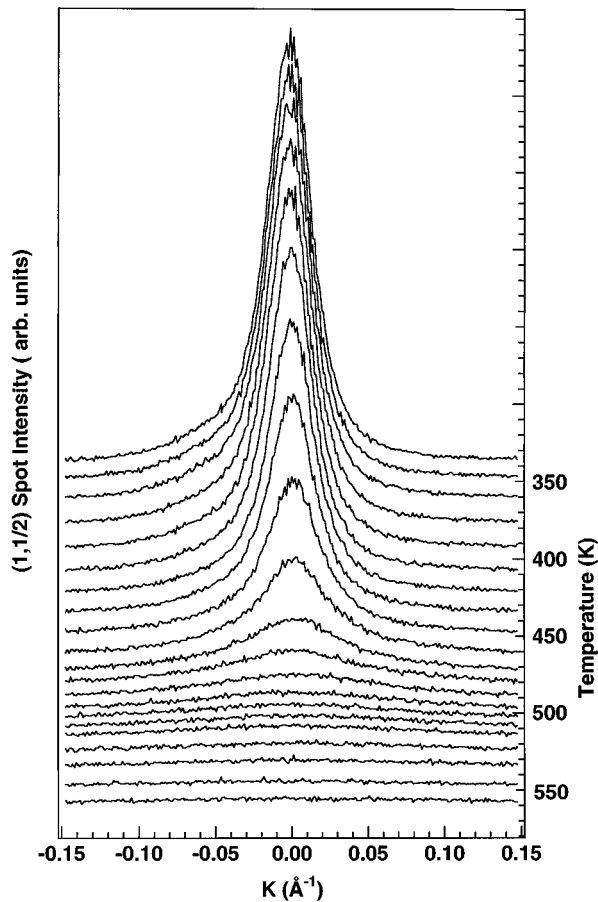


FIG. 1. Spot profiles measured along the [01] direction at an energy of 58 eV, as a function of temperature.

1×10^{-8} mbar) at 1070 K. The sample was then flashed to 1200 K and, while cooling, reduced in hydrogen (5×10^{-7} mbar) in order to remove any residual oxygen. X-ray photoemission spectroscopy (XPS) has shown that this cleaning procedure results in a C- and O-free surface,^{6,7} and a sharp (1×1) LEED pattern is obtained. The average (1×1) island size was evaluated from the full width at half maximum (FWHM) of a diffraction spot, and was greater than 500 Å in both main crystallographic directions.

Immediately before oxygen exposure, the sample was flashed to 600 K to remove any residual adsorbed hydrogen or CO. The $p(2 \times 2)$ oxygen overlayer was obtained by exposing the clean Rh surface to 0.65 L (1 L = 1.3×10^{-6} mbar s) of O_2 at room temperature. To compensate for oxygen loss due to a reaction with hydrogen from the ambient, oxygen was left flowing during the experiments (pressure in the 10^{-10} -mbar range) to maintain a constant coverage. The flow was calibrated by adjusting the partial pressure until the peak intensity at a chosen temperature remained the same after a heating/cooling cycle. The SPA-LEED was operated at 58-eV electron-beam energy, which corresponds roughly to maxima for the $(\frac{1}{2}, \frac{1}{2})$ and $(1, \frac{1}{2})$ spot intensities.

III. RESULTS

A typical sequence of spectra for the $(1, \frac{1}{2})$ spot is presented in Fig. 1. The data were collected by recording the

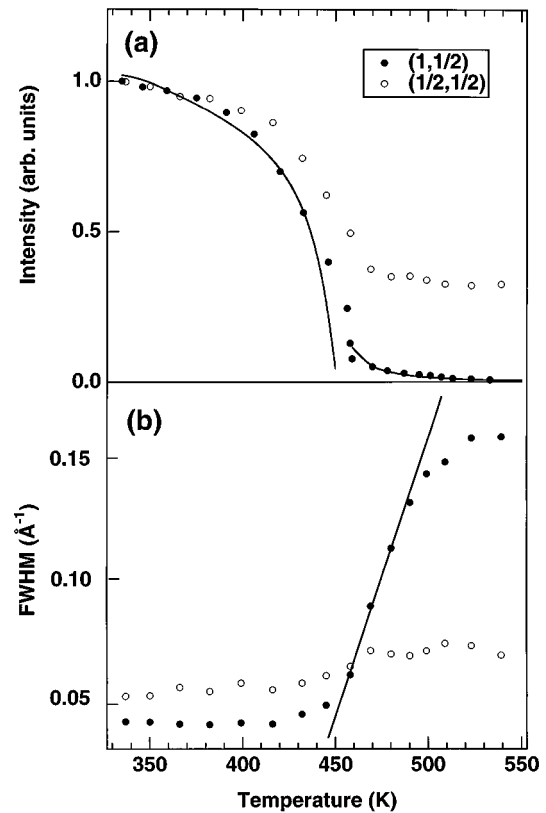


FIG. 2. (a) Peak intensity of the $(1, \frac{1}{2})$ and $(\frac{1}{2}, \frac{1}{2})$ spots as a function of temperature. The full line is a fit of a power law $|t|^{2\beta}$ for $t < 0$ and $|t|^{-\gamma}$ for $t > 0$, where t is the reduced temperature (see text). (b) Full width at half maximum (along the [01] direction) of the $(1, \frac{1}{2})$ and $(\frac{1}{2}, \frac{1}{2})$ spots. Symbols as in (a). The full line is a fit of a power law $|t|^\nu$ of the region close to the transition (see text)

spot profile at different temperatures while slowly heating the $p(2 \times 2)$ overlayer.

In Fig. 2 are plotted the peak intensity and peak width against sample temperature for the $(1, \frac{1}{2})$ and $(\frac{1}{2}, \frac{1}{2})$ spots. The peak intensity (defined as the peak maximum) and width (defined as full width half maximum) have been obtained by fitting the spot profiles with a convolution of a Lorentzian and a Gaussian function, after background subtraction (obtained by a linear fit of the tails of the peaks). All data have been corrected for the Debye-Waller attenuation factor, determined by fitting the spot intensity decay well below the transition temperature, in a range between 170 and 270 K. It is clearly seen in Fig. 2 that the two peaks behave differently. The $(1, \frac{1}{2})$ spot, characteristic of the $p(2 \times 2)$ pattern only, shows a sharp drop in intensity around 450 K and it vanishes above 500 K. The $(\frac{1}{2}, \frac{1}{2})$ spot also drops in intensity around 450 K but does not disappear, and stays constant up to the highest temperature measured (650 K).

The drop in intensity of the $(1, \frac{1}{2})$ spot is accompanied [see Fig. 2(b)] by a broadening of the peak from 0.04 \AA^{-1} below the transition to about 0.16 \AA^{-1} above it, whereas the $(\frac{1}{2}, \frac{1}{2})$ peak width stays nearly constant. We therefore interpret the data as a $p(2 \times 2) \rightarrow c(2 \times 2)$ second-order phase transition. The fact that the $(\frac{1}{2}, \frac{1}{2})$ spots remain is entirely consistent with symmetry requirements, as a $p(2 \times 2) \rightarrow p(1 \times 1)$ transition, for instance, cannot be second order.¹⁹

By fitting the data in Fig. 2, it is possible to determine the

TABLE I. Comparison between theoretical (2D Ising) and experimental values for the critical exponents of the $p(2 \times 2) \rightarrow c(2 \times 2)$ order-disorder transition.

Exponent	Theory (2D Ising)	Experiment
β	0.125	0.120 ± 0.008
γ	1.75	1.70 ± 0.20
ν	1	1.01 ± 0.12
α	0	0.04 ± 0.12

critical exponents β , γ , and ν of the transition, related respectively to the order parameter, susceptibility and correlation length.^{10,11} The values of β , γ , and ν unequivocally identify the universality class to which the transition belongs. The fitting procedure was as follows.

First, the peak width broadening of the $(1, \frac{1}{2})$ peak was fitted by a power law $|t|^p$, where t is the reduced temperature, defined as $(T - T_c)/T_c$. Second, β was evaluated by fitting the spot intensity below the critical temperature T_c (obtained by the previous step) with $|t|^{2\beta}$. Finally, the spot intensity above T_c , fitted by $|t|^{-\gamma}$, yielded γ . We obtained a value of 450 ± 5 K for T_c , and for β , γ , and ν the values reported in Table I, which are in very good agreement with the values predicted by the 2D Ising model. The errors associated with the estimated values are the statistical errors of the fit, taking into account the uncertainties of the single data points.

The curves resulting from the fitting procedure are superimposed on the experimental data in Fig. 2. The deviation of the fit curve from the measured peak width curve at high temperatures can be attributed to an experimental artifact, as at high temperatures the peak broadens beyond the experimental k range used to measure the peak shape, and therefore the width is systematically underestimated. This problem is aggravated by the fact that the intensity has dropped considerably and it is not easy to estimate the peak width (see Fig. 1). For this reason the fit of this curve has been performed in a limited temperature range ($T < 500$ K).

It is possible to obtain an independent confirmation of the universality class to which the transition belongs (and of the value of T_c) by determining the value of the parameter α which gives the best agreement with the data. This can be obtained by fitting the temperature dependence of the peak area (rather than the peak height used before) to the expression

$$I(T) = A \mp B_{\pm} |t|^{1-\alpha} - A_1 t + \dots,$$

where \pm refers to T larger or smaller than T_c , respectively.¹⁰ Experimental data and the fit are reported in Fig. 3. The value of the α parameter obtained from the fit, reported in Table I, is found to depend strongly on the temperature range around T_c used in the fitting procedure. This variation has been included in the error associated with α . Within this error, good agreement with the 2D Ising value is achieved.

IV. DISCUSSION

When the domain diameter is smaller than the transfer width, as it is in our system, superposition of the diffraction

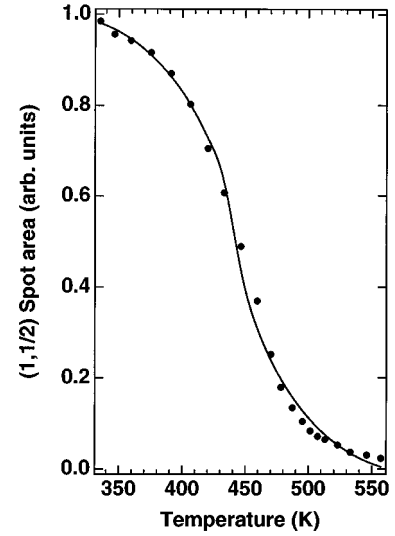


FIG. 3. Integrated intensity of the $(1, \frac{1}{2})$ spot; full line: fit with equation $I(T) = A \mp B_{\pm} |t|^{1-\alpha} - A_1 t$, see text.

amplitudes due to domains of different phase causes broadening of the diffraction spots. As noted above, point defects do not cause broadening, so we can exclude these as a source of our experimental line broadening. The defects generated in the phase transition are responsible both for the destruction of long-range order, which goes to zero at the critical temperature, and for the broadening of the $(1, \frac{1}{2})$ spots. The type of extended defects involved in the present line broadening can be labeled with surface Burgers vectors.¹⁴ The condition for broadening to occur is¹⁴

$$\Delta \mathbf{k} \cdot \mathbf{b} \neq 2n\pi,$$

where $\Delta \mathbf{k}$ is the wave number change of the scattered beam, and \mathbf{b} is the Burgers vector.

For the $(1, \frac{1}{2})$ spots, we can write the diffraction vector in three dimensions as

$$\mathbf{G} = \frac{2\pi}{a'} (0, 1, \frac{1}{2}),$$

where a' is the (1×1) surface lattice parameter, equal to $a/\sqrt{2}$, and a is the conventional lattice parameter. Then broadening may be caused by defects with Burgers vectors of type

$$\mathbf{b} = a' [001], \quad \mathbf{b} = a' [011] \quad \text{and} \quad \mathbf{b} = a' [0\bar{1}\bar{1}].$$

(We have introduced the bars to indicate defects which are commonly called light walls, i.e., one in which the local stoichiometry is reduced.) Examples of these defects (commonly denoted domain walls) are illustrated in Fig. 4. For the $p(2 \times 2)$ structure, defects with $\mathbf{b} = a' [011]$ and $\mathbf{b} = a' [0\bar{1}\bar{1}]$ [see Figs. 4(b) and 4(c)] do not cause broadening of the $(\frac{1}{2}, \frac{1}{2})$ spot: only the other type does so. This is clear from the broadening condition above

$$\Delta \mathbf{k} \cdot \mathbf{b} = \frac{2\pi}{a'} a' [k_z, \frac{1}{2}, \frac{1}{2}] \cdot [0, 1, 1] = 2\pi.$$

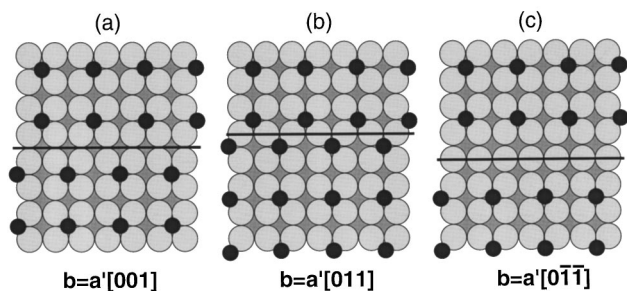


FIG. 4. Structure models of defects with their corresponding surface Burgers vectors.

The stronger broadening of the $(1, \frac{1}{2})$ spot compared with $(\frac{1}{2}, \frac{1}{2})$ is taken to indicate that indeed defects of type $\mathbf{b} = a'[011]$ or $\mathbf{b} = a'[0\bar{1}\bar{1}]$ cause the observed broadening:

$$\Delta \mathbf{k} \cdot \mathbf{b} = \frac{2\pi}{a'} a' [k_z, 1, \frac{1}{2}] \cdot [0, 1, 1] = 3\pi \neq 2n\pi.$$

However, no shift of the fractional-order spots was observed, an effect which can be used to distinguish between the two types of defects (b) and (c).¹⁶ It is therefore concluded that there are equal numbers of these defects, or that they are decorated with extra atoms in such a way that neither one pure type nor the other occurs.

The broadening of the diffraction spots with increasing temperature is symmetric in both the (10) and (01) crystallographic directions, as expected for a (100) surface. No splitting of the diffraction spots was observed, indicating that there is no preferential domain size. The mean width of the $p(2 \times 2)$ domains varies from 160 Å at 370 K to 30–40 Å above the transition temperature T_c .

The domain size at low temperature is determined by defects which occur during formation. It has been shown that the critical temperature can be corrected approximately for these finite-size effects:^{22,23}

$$\Delta T = aL^{-\nu} T_c,$$

where ΔT is the reduction in measured critical temperature from the ideal T_c , a is a constant ~ 1.25 , and L is the domain size in lattice constants of the (1×1) substrate. Since in our case $\nu = 1$, this yields a correction of ~ 10 K.

For a pure Ising transition of the type $p(2 \times 2) \rightarrow c(2 \times 2)$, the $(\frac{1}{2}, \frac{1}{2})$ spot should not broaden at all. In real-

ity, some slight broadening from the initial value does occur. This is assigned to the finite quality of the sample, i.e., the presence of some steps or slight deviation from stoichiometry.

The transition can also be considered from the point of view of energetics. For a q -state Potts model, a square lattice and $J > 0$ (attractive interaction), the critical temperature is given by the condition

$$\left[\exp\left(\frac{J}{K_B T_c}\right) - 1 \right]^2 = q,$$

where K_B is the Boltzmann constant, and J is an energy.¹⁰

The value of q is 2 for a 2D Ising phase transition, giving a value of J equal to 43 ± 2 meV/atom. This represents the energy/atom of the fundamental excitation involved in the loss of order of the system. The fact that the exponents agree so well with the Ising values supports the basic assumption of the Ising model that nearest-neighbor interaction is dominant. We therefore identify J with the interaction energy per atom at the core of the defect, due to the fact that the local environment is no longer that of the ordered $p(2 \times 2)$. Furthermore, this gives directly the energy per unit length of the defect, which is $43/2.87 \times 2 = 7.5$ meV/Å. To our knowledge few experimental determinations of the energy J have been performed, so it is difficult to compare our result with the literature. In any case, a value of 0.2 eV/atom was determined for the order-disorder transition on Si(111),²⁴ while Roelofs *et al.*²⁵ calculated energies of just 2–10 meV/atom for defects on Au(110). The chemical bonding of these two clean surfaces is rather different from that in the present adsorbate system, but the energy is of the same order of magnitude.

V. CONCLUSION

We have demonstrated that the oxygen induced $p(2 \times 2)$ structure on Rh(100) undergoes a phase transition to a $c(2 \times 2)$ structure. This transition belongs to the two-dimensional Ising universality class. By careful analysis of diffraction profile data we have been able to define the type of defect which proliferates at the critical temperature. Thermodynamic analysis permits the association of an energy per unit length with this defect, which is thus crystallographically and energetically defined.

*Present address: I.R.C. in Surface Science, University of Liverpool, Liverpool L69 3BX, UK.

†Also at Dipartimento di Fisica, Università di Trieste, I-34127 Trieste.

¹L. H. Dubois, *J. Chem. Phys.* **15**, 5228 (1982).

²W. Oed, B. Dotsch, L. Hammer, K. Heinz, and K. Müller, *Surf. Sci.* **207**, 55 (1988).

³C. W. Tucker, *J. Appl. Phys.* **37**, 3013 (1966).

⁴D. G. Castner, B. A. Sexton, and G. A. Somorjai, *Surf. Sci.* **71**, 519 (1978).

⁵W. H. Daniel, Y. Kim, H. C. Peebles, and J. M. White, *Surf. Sci.* **111**, 189 (1981).

⁶L. Gregoratti, A. Baraldi, V. R. Dhanak, G. Comelli, M. Kiskinova and R. Rosei, *Surf. Sci.* (to be published).

⁷A. Baraldi, L. Gregoratti, G. Comelli, V. R. Dhanak, M. Kiskinova, and R. Rosei, *Appl. Surf. Sci.* (to be published).

⁸J. R. Mercer, P. Finetti, F. M. Leibsle, V. R. Dhanak, R. McGrath, A. Baraldi, K. C. Prince, and R. Rosei, *Surf. Sci.* (to be published).

⁹M. Zacchigna, C. Astaldi, K. C. Prince, M. Sastry, C. Comincioli, R. Rosei, C. Quaresima, C. Ottaviani, C. Crotti, A. Antonini, M. Matteucci, and P. Perfetti, *Surf. Sci.* (to be published).

¹⁰E. Bauer, in *Chemisorbed Layers, Structures and Dynamics of Surfaces II*, edited by W. Schommers and P. von Blanckenhagen (Springer-Verlag, Berlin, 1987).

¹¹B. N. J. Persson, *Surf. Sci. Rep.* **15**, 1 (1992).

¹²J. C. Campuzano, M. S. Foster, G. Jenning, R. F. Willis, and W. Unertl, *Phys. Rev. Lett.* **54**, 2684 (1985).

- ¹³T. Schneider and E. Stoll, Phys. Rev. B **13**, 1216 (1976); see also A. D. Bruce and R. A. Cowley, *Structural Phase Transition* (Taylor & Francis, London, 1981).
- ¹⁴K. C. Prince, A. Morgante, D. Cvetko, and F. Tommasini, Surf. Sci. **297**, 235 (1993).
- ¹⁵A. F. Bellman, D. Cvetko, A. Morgante, M. Polli, F. Tommasini, K. C. Prince, and R. Rosei, Surf. Sci. **281**, L321 (1993).
- ¹⁶P. Fenter and T.-M. Lu, Surf. Sci. **154**, 15 (1985).
- ¹⁷G.-C. Wang and T.-M. Lu, Phys. Rev. B **31**, 5918 (1985).
- ¹⁸P. Piercy and H. Pfnür, Phys. Rev. Lett. **59**, 1124 (1987).
- ¹⁹S. Deonarain and J. L. Birman, Phys. Rev. B **27**, 2855 (1983).
- ²⁰U. Scheithauer, G. Mayer, and M. Henzler, Surf. Sci. **178**, 534 (1986).
- ²¹V. R. Dhanak, A. Baraldi, and K. C. Prince (unpublished).
- ²²A. E. Ferdinand and M. E. Fisher, Phys. Rev. **185**, 832 (1969).
- ²³D. P. Landau, Phys. Rev. B **13**, 2997 (1976).
- ²⁴M. Wautelet, Surf. Sci. **187**, L655 (1987).
- ²⁵L. D. Roelofs, S. M. Foiles, M. S. Daw, and M. I. Baskes, Surf. Sci. **234**, 63 (1990).